

Part V

Special topics



# 22

## Small-amplitude surface waves

Surface waves in the sea are created by the interaction of wind and water which somehow transforms the steady motion of the streaming air into the nearly periodic swelling and subsiding of the water. The waves appear to roll towards the coast in fairly orderly sequence of crests and troughs that is translated into the quick ebb and flow of water at the beach, so well-known to all of us. On top of that there is of course the slow ebb and flow of the tides.

In constant “flat-earth” gravity, the interface between two fluids at rest is always horizontal. In moving fluids the interface can take a very complex instantaneous shape under the simultaneous influence of inertia, pressure, gravity, container shape, surface tension, and viscosity. Waves controlled by pressure and gravity are naturally called *gravity waves*, whereas waves controlled by pressure and surface tension are called *capillary waves*. If the fluids have vastly different densities, as is the case for the sea and the atmosphere, one may often disregard the lighter fluid and instead consider the open surface of the heavier fluid towards vacuum. For fluids of nearly equal density, for example a saline bottom layer in the sea with a brackish layer above, *internal gravity waves* driven by pressure and buoyancy may arise in the interface.

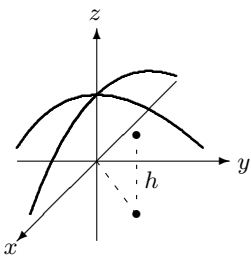
This chapter is devoted to the various types of small-amplitude surface waves and the conditions under which they occur (see [58, 59, 40, 16, 9] for extended discussions of surface waves). Mathematically, small-amplitude waves are by far the most easy to deal with. More interesting and unusual wave types arise when amplitudes grow so large that the nonlinear aspects of fluid mechanics come into play. Nonlinear waves are common everyday occurrences, for example the familiar run-up of waves on a beach or the less familiar sonic boom from an aircraft overhead, but the subject of nonlinear waves is unfortunately so mathematically challenging that we shall postpone it until chapter 30.

## 22.1 Basic physics of surface waves

In chapter 7 we saw that the shape of an interface between two fluids in hydrostatic equilibrium is determined by the balance between the pressure gradient and gravity everywhere in the interior of the fluids. Surface tension in the interface may also have profound influence on the shape of small fluid volumes, for example a raindrop. What we shall call waves in this chapter are time-dependent disturbances in the shape of an interface originally in hydrostatic equilibrium.

Although surface waves may occur wherever material properties change rapidly, we shall mostly think of gravity waves in water so well-known to all of us. In constant gravity, the hydrostatic interface between the sea and the air is flat and horizontal, usually taken to be  $z = 0$  in the flat-earth coordinate system. A wave will disturb the surface so that its instantaneous height is a function of the horizontal coordinates and time,

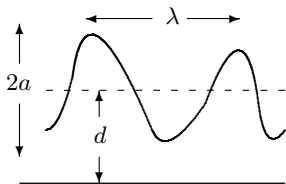
$$z = h(x, y, t) . \quad (22-1)$$



A surface wave in the flat-earth coordinate system.

We shall mainly be interested in trains of waves that progress periodically and in a regular pattern across the horizontal surface of the sea, although everyday experience tells us that waves may be much more complicated. In a breaking wave, the surface height is not even a single-valued function of position and time.

Waves can be created in many ways. The splash you make when you jump bottom-first into a swimming pool creates primarily a single large ring-shaped wave, perhaps followed by several smaller waves. When these waves hit the edge of the pool they are reflected and interfere with themselves to create quite chaotic patterns. In this chapter we shall, however, not be concerned much with the mechanisms by which waves are created, but rather with their internal dynamics after they have somehow been brought into existence.



A general wave consists of mounds and hollows. Locally, the amplitude  $a$  is related to the vertical distance between maxima and minima, the wavelength  $\lambda$  to the horizontal size of a mound or hollow, and the period  $\tau$  to the time scale for major changes in the local pattern. The depth  $d$  to the vertical distance to the bottom.

### Wave parameters

Any non-breaking surface wave consists locally of mounds and hollows of roughly the same size in the otherwise smooth equilibrium surface. Although a general wave can be very complex, it is convenient to describe these local features in terms of parameters that normally are reserved for harmonic waves:

- $a$  — amplitude. It sets the scale for vertical variations in the height of the wave. Mostly it is taken to be the height of a mound above the equilibrium level, or equivalently the depth of a hollow below.
- $\lambda$  — wavelength. This is the horizontal length scale of the wave, typically related to the width of a mound or a hollow.
- $\tau$  — period. A measure of the time scale for major changes in the wave pattern, for example the time it takes for a mound to become a hollow
- $d$  — depth. The vertical distance to a solid boundary, the “bottom”.

The ratio  $c = \lambda/\tau$  is called the *celerity* or *phase velocity* and characterizes the speed with which the waveform changes shape.

If the wavelength is much greater than the depth,  $\lambda \gg d$ , we shall speak about *long waves* or more graphically *shallow-water waves*. Similarly, waves with wavelength much smaller than the depth,  $\lambda \ll d$ , are called *short waves* or *deep-water waves*. Waves with amplitude much smaller than both wavelength and depth,  $a \ll \lambda, d$ , are called a *small-amplitude* waves.

### The dispersion law

In a gravity wave the force of gravity pulls the water in a mound downwards and sets it into motion, and this motion may in turn make the water rise again. Whereas the potential energy of the wave only depends on its shape, the kinetic energy also depends on the flow velocities in the wave, and thus on the period. Therefore, if no energy is lost to friction, this continual conversion of potential energy into kinetic energy and back must provide a relation between the period of a wave and the other parameters,

$$\tau = \tau(a, \lambda, d, \dots). \quad (22-2)$$

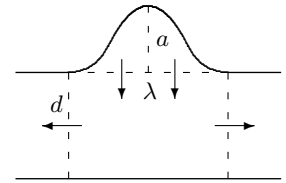
The precise form of this *dispersion law* for a particular type of wave is normally obtained from careful analysis of the wave dynamics, several examples of which will be given later. Here we shall only make a coarse estimate of the general form of the dispersion law using that potential and kinetic energies must be of comparable magnitudes.

### Collapse of a “waterberg”

Suppose we have somehow created a mound of water, instantaneously at rest, for example by pulling an inverted water-filled bucket up through the flat surface of the sea. Common experience tells us that such a “waterberg” will quickly collapse into the sea, creating instead a smaller and wider hollow which may later rise again to make an even smaller mound that in turn collapses, and so on. Eventually all traces of the initial mound will have disappeared into secondary waves running away over the surface.

Let the initial mound have height  $a$  and width  $\lambda$  so that its volume is of magnitude  $\lambda^2 a$ . During the first collapse all the water in the mound will move vertically downwards and reach the sea level in a characteristic time  $\tau$ . Since water is incompressible, an equal volume has to move horizontally away from the collapse region with a typical speed  $U$ . For long waves with  $\lambda \gg d$ , the proximity of the bottom forces all the water underneath the mound to move away horizontally, so that  $\lambda^2 a \sim \lambda d U \tau$ . Solving for  $U$  we find

$$U \sim \frac{a\lambda}{\tau d}. \quad (22-3)$$



A “waterberg” of height  $a$  and width  $\lambda$  rising out of a sea of depth  $d$ . When the waterberg collapses vertically, all the water in it has to leave in the horizontal directions.

Since the typical vertical speed is  $a/\tau$ , the horizontal flow velocity in a shallow sea will be much greater than the vertical by a factor  $\lambda/d \gg 1$ . For short waves with  $\lambda \ll d$ , there is no bottom to divert the water flow so that the horizontal velocity tends to be of same order of magnitude as the vertical, *i.e.*  $U \sim a/\tau$  near the surface. From the expression for  $U$ , one may thus conclude that the deep sea may be characterized by an effective depth of the same magnitude as the wavelength,  $d \sim \lambda$ . These claims will later be confirmed by precise calculations, showing in fact that the effective depth of the deep sea is  $d \approx \lambda/2\pi$ .

The potential energy of the initial mound relative to the general level of the sea is of magnitude,

$$\mathcal{V} \sim \rho_0 \lambda^2 a \cdot g_0 a = \rho_0 g_0 a^2 \lambda^2 . \quad (22-4)$$

Interestingly, a hollow of depth  $a$  and width  $\lambda$  would have potential energy of the same magnitude, for the simple reason that buoyancy presses the surface upward, like the hull of a ship.

The kinetic energy of the volume of water of size  $\lambda^2 d$  under the wave becomes of magnitude

$$\mathcal{T} \sim \rho_0 \lambda^2 d \cdot U^2 \sim \rho_0 \frac{\lambda^4 a^2}{\tau^2 d} . \quad (22-5)$$

In the absence of dissipation, the kinetic energy must be comparable to the potential energy,  $\mathcal{T} \sim \mathcal{V}$ , and solving for  $\tau$  we obtain the estimate of the dispersion law,

$$\boxed{\tau \sim \frac{\lambda}{\sqrt{g_0 d}}} . \quad (22-6)$$

Notice that this dispersion law is merely a coarse estimate of the overall magnitude of the collapse time. It may still be multiplied with an unknown factor of order unity which can depend on the dimensionless ratios  $a/\lambda$  and  $d/\lambda$ , and possibly on other dimensionless parameters characterizing the actual shape of the wave.

From the dispersion law we immediately get the phase velocity

$$c = \frac{\lambda}{\tau} \sim \sqrt{g_0 d} . \quad (22-7)$$

Like an echo of Toricelli's law (page 266) it is of the same order of magnitude as the free-fall velocity  $\sqrt{2g_0 d}$  from height  $d$ . In shallow water where  $d$  is the true depth of the sea, the phase velocity is independent of wavelength. In deep water where the true depth is infinite, the effective depth may as pointed out above be taken to be  $d \approx \lambda/2\pi$ .

**Example 22.1.1:** A little “waterberg” created by lifting an inverted bucket of height  $a = 30$  cm and width  $\lambda = 50$  cm out of water of depth  $d = 1$  m collapses in  $\tau \sim 0.1$  s, a mere blink of the eye.

### Gravity waves are nearly ideal

The shape of a surface wave is only a manifestation of the (literally) underlying hydrodynamics, governed by the Navier-Stokes equations. From the estimate (22-3) of the horizontal flow velocity we estimate the Reynolds number in shallow water to be,

$$\text{Re} = \frac{|(\mathbf{v} \cdot \nabla)\mathbf{v}|}{\nu |\nabla^2 \mathbf{v}|} \sim \frac{U^2/\lambda}{\nu U/d^2} = \frac{ad}{\nu\tau}. \quad (22-8)$$

Here we have assumed that the advective acceleration is dominated by the fast horizontal motion over a length scale  $\lambda$ , whereas the viscous acceleration is dominated by the vertical variation in the horizontal flow over the depth  $d$ . For deep-water waves  $d$  may as before be replaced by  $\lambda/2\pi$ .

The typical sea waves we encounter when swimming close to the shore at a depth of a couple of meters have amplitudes up to a meter and periods of some seconds. With  $\nu \approx 10^{-6} \text{ m}^2/\text{s}$  for water, the Reynolds number will be in the millions, and viscosity plays essentially no role for such waves. In daily life we are otherwise quite familiar with viscous waves, for example while stirring porridge, but they are not so interesting because they quickly die out. Nearly ideal gravity waves in water simply keep rolling along. Eventually viscosity will also make these waves die away if left on their own, but that problem can be dealt with separately (see section 22.6).

### Small-amplitude waves are nearly linear

The nonlinearity of the equations of fluid mechanics makes surface waves much more complex than, for example, electromagnetic waves governed by the linear Maxwell equations. The nonlinear advective acceleration of the fluid  $(\mathbf{v} \cdot \nabla)\mathbf{v}$  can however often be disregarded in comparison with the local acceleration  $\partial\mathbf{v}/\partial t$ , so that the Navier-Stokes equations also become linear. For shallow-water waves we obtain the ratio of advective to local acceleration,

$$\frac{|(\mathbf{v} \cdot \nabla)\mathbf{v}|}{|\partial\mathbf{v}/\partial t|} \approx \frac{U^2/\lambda}{U/\tau} \approx \frac{U}{c} \approx \frac{a}{d}. \quad (22-9)$$

Quite generally we can conclude that the advective term plays no role for small-amplitude waves with  $a \ll d$  (with  $d \approx \lambda/2\pi$  in deep water). In short: *the Navier-Stokes equations become linear in the small-amplitude limit.*

The most general solution to a set of linear field equations with constant coefficients is a linear superposition of elementary harmonic solutions (possibly damped). We have seen this for small-amplitude vibrations in solids (chapter 13) as well as for small-amplitude pressure waves in fluids (section 18.6). In these cases the three-dimensional waves are superpositions of elementary plane waves, each of which at any given time has constant physical properties in any plane orthogonal to its direction of propagation. The same will be the case for the flow underlying small-amplitude surface waves.

### Harmonic line waves

Three-dimensional plane waves have identical physical properties in every plane orthogonal to the direction of propagation. Surface waves are two-dimensional, and elementary harmonic surface waves have correspondingly the same physical properties on any line orthogonal to the direction of propagation. A harmonic *line wave* is of the form

$$h = a \cos(k_x x + k_y y - \omega t + \chi) \quad (22-10)$$

where  $\mathbf{k} = (k_x, k_y, 0)$  is *wave vector*,  $k = |\mathbf{k}| = 2\pi/\lambda$  the *wave number*,  $\omega = 2\pi/\tau$  the *circular frequency*, and  $\chi$  the *phase shift*. The argument of the cosine,  $\phi = k_x x + k_y y - \omega t + \chi$ , is called the *phase* of the wave. The phase shift can for a single wave always be absorbed in the choice of origin of the coordinate system or of time, but differences between phase shifts may become of physical importance when waves are superposed.

The maxima or minima, or *crests* and *troughs* as they are called for surface waves, move steadily along in the direction  $\mathbf{n} = \mathbf{k}/k = (\cos \theta, \sin \theta, 0)$  with the *phase velocity*,

$$c = \frac{\lambda}{\tau} = \frac{\omega}{k}. \quad (22-11)$$

For small-amplitude shallow-water waves where the dispersion law is linear, the phase velocity is independent of the wave number  $k$ . In general, however, the dispersion law will be nonlinear,  $\tau = \tau(\lambda)$  or equivalently  $\omega = \omega(k)$ , as we saw for deep-water waves, and the phase velocity will depend on the wave number.

### Group velocity

Consider now two harmonic line waves which for simplicity are chosen to run along the  $x$ -axis with the same amplitudes. Their phases are  $\phi_1 = k_1 x - \omega_1 t + \chi_1$  and  $\phi_2 = k_2 x - \omega_2 t + \chi_2$ , and using the trigonometric relation,

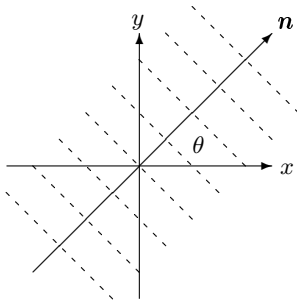
$$\cos \phi_1 + \cos \phi_2 = 2 \cos \frac{\phi_1 + \phi_2}{2} \cos \frac{\phi_1 - \phi_2}{2}, \quad (22-12)$$

the superposition  $h = h_1 + h_2$  may be written,

$$h = 2a \cos(kx - \omega t + \chi) \cos \frac{1}{2}(\Delta k x - \Delta \omega t + \Delta \chi), \quad (22-13)$$

where  $k = (k_1 + k_2)/2$  etc are the average quantities for the two waves, and  $\Delta k = k_1 - k_2$  etc are the differences. The first oscillating factor evidently describes a line wave moving along the  $x$ -axis with the average values of the wave numbers, frequencies, and phase shifts, but the amplitude of this wave is now *modulated* by the second factor.

If the differences are much smaller than the averages,  $|\Delta k| \ll |k|$ ,  $|\Delta \omega| \ll |\omega|$ , and  $|\Delta \chi| \ll |\chi|$ , the second cosine factor will only slowly modulate the rapid



A periodic line wave on the surface. The crests are parallel lines orthogonal to the vector  $\mathbf{n} = (\cos \theta, \sin \theta, 0)$ , forming an angle  $\theta$  with the  $x$ -axis.

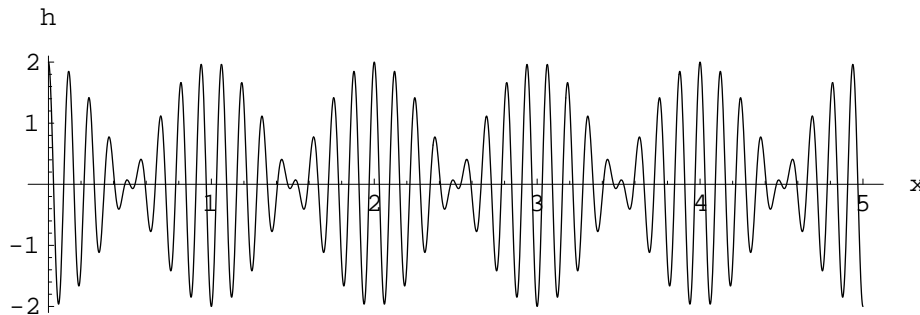


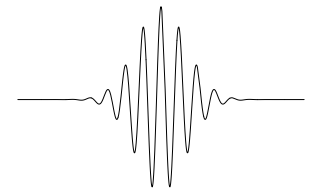
Figure 22.1: Superposition of two harmonic line waves with nearly equal wave numbers, here at  $t = 0$  for  $k = 8\Delta k$ ,  $\Delta k = 2\pi$ ,  $a = 1$ , and  $\chi = 0$ . The rapid oscillations of the “carrier” wave is modulated and broken into a “beat pattern” of wave packets of length  $2\pi/\Delta k = 1$  centered at  $x = n$  for all integer  $n$ .

oscillations of the first. Since the second cosine vanishes when its arguments passes through  $\frac{1}{2}\pi + n\pi$  where  $n$  is an arbitrary integer, it will chop the average wave up into a string of *wave packets* of typical length  $L = 2\pi/|\Delta k|$ , as pictured in fig. 22.1. Inside each wave packet, the crests will move with the phase velocity  $c = \omega/k$ , whereas the center of each wave packet will move with the speed  $\Delta\omega/\Delta k = (\omega(k_1) - \omega(k_2))/\Delta k \approx d\omega(k)/dk$ . Thus, the propagation speed of a wave packet is given by the derivative of the dispersion law,

$$c_g = \frac{d\omega}{dk}, \quad (22-14)$$

called the *group velocity*.

Any superposition of waves with nearly equal wave vectors will in fact form one or more wave packets moving with the group velocity (see problem 22.1). If the dispersion law is linear, the group and phase velocities are equal, but if the dispersion law is non-linear they will be different, and the waves are said to be *dispersive*. If the group velocity is smaller than the phase velocity,  $c_g < c$ , the wave crests will move forward inside a wave packet as it proceeds across the surface, and conversely if it is larger.



A single Gaussian wave packet.

## Energy transport and group velocity

In a single wave packet, the velocity field is only non-zero in the region covered by the wave packet, so that the energy of the wave must be concentrated here and transported along the surface with the group velocity, rather than with the phase velocity. The same must be true for any superposition of single wave packets with wave numbers taken from a narrow band of width  $\Delta k$  around  $k$ , such as the one shown in fig. 22.1. In the limit where the bandwidth  $\Delta k$  narrows down to nothing, the energy must still be transported with the group velocity, so in the end we reach the slightly strange conclusion, that even in a purely monofrequent line wave, the energy must be transported with the group velocity. This will be shown explicitly to be true in section 22.3.

## 22.2 Small-amplitude gravity waves

Small-amplitude, inviscid gravity waves in incompressible water obey a linear version of Euler's equation,

$$\frac{\partial \mathbf{v}}{\partial t} = -\frac{1}{\rho_0} \nabla p + \mathbf{g}, \quad \nabla \cdot \mathbf{v} = 0, \quad (22-15)$$

where  $\mathbf{g} = (0, 0, -g_0)$ . These equations do not explicitly involve the surface height, which will only come in via the boundary conditions.

### Boundary conditions

At the open surface,  $z = h$ , there are two boundary conditions which must be fulfilled. The first is purely kinematic and expresses that a fluid particle sitting on the surface should follow the surface motion. Under the assumption of small amplitudes,  $a \ll d, \lambda$ , the surface is nearly horizontal everywhere, so that the vertical velocity of the fluid just below the surface should equal the vertical velocity of the surface itself (see chapter 30 for the general condition),

$$\frac{\partial h}{\partial t} = v_z \quad \text{for } z = h. \quad (22-16)$$

The second boundary condition is dynamic and expresses the continuity of the pressure across the surface. Assuming that there is air or vacuum with constant pressure  $p_0$  above the surface, the condition becomes

$$p = p_0 \quad \text{for } z = h. \quad (22-17)$$

Here we have disregarded surface tension which would add a contribution to the right hand side (see section 8.1).

Besides these, there will be further boundary conditions that depend on the shape of the container.

### Velocity potential

The time derivative of the velocity field  $\partial \mathbf{v} / \partial t$  is evidently a gradient field, so if the velocity field initially is a gradient field, it will keep on being one. Thus, in view of the linearity, the most general solution to the field equations is an irrotational (gradient) field superposed with a constant field, possibly containing vorticity. We shall from now on focus on the time dependent irrotational component and write it as the gradient of the *velocity potential*  $\Psi$ , which due to the divergence condition has to satisfy Laplace's equation (see section 16.6),

$$\mathbf{v} = \nabla \Psi, \quad \nabla^2 \Psi = 0. \quad (22-18)$$

Inserting this into the field equation and solving for the pressure, we find

$$p = p_0 - \rho_0 \left( g_0 z + \frac{\partial \Psi}{\partial t} \right). \quad (22-19)$$

Here  $p_0$  could in principle be an arbitrary function of time which we shall chose to be equal to the pressure at the open surface. With this choice we obtain

$$\frac{\partial h}{\partial t} = \nabla_z \Psi, \quad g_0 h = -\frac{\partial \Psi}{\partial t} \quad \text{for } z = h \quad (22-20)$$

from the open surface boundary conditions.

### Harmonic line wave solution

Suppose now that the surface wave is an elementary harmonic line wave in the  $x$ -direction,  $h = a \cos(kx - \omega t)$ , so that the flow underneath can be assumed to be everywhere independent of  $y$ . From the kinematic condition (22-16), it follows that  $\nabla_z \Psi = a\omega \sin(kx - \omega t)$  for  $z = h$ . This suggests that the velocity potential at all depths will be of the form

$$\Psi = f(z) \sin(kx - \omega t), \quad (22-21)$$

where  $f(z)$  is a so far unknown function of  $z$ . The Laplace equation (22-18) takes here the form  $\nabla_z^2 \Psi = -\nabla_x^2 \Psi$  and leads immediately to  $f'' = k^2 f$ . The most general solution to this equation is

$$f(z) = Ae^{kz} + Be^{-kz} \quad (22-22)$$

where  $A$  and  $B$  are constants to be determined from the boundary conditions.

### Deep-water waves

In deep water the velocity field must be finite for  $z \rightarrow -\infty$ , implying that  $B = 0$  so that  $f(z) = Ae^{kz}$ . The open surface boundary conditions (22-20) now lead to,

$$\begin{aligned} a\omega \sin(kx - \omega t) &= k A e^{kh} \sin(kx - \omega t) \\ g_0 a \cos(kx - \omega t) &= \omega A e^{kh} \cos(kx - \omega t) \end{aligned}$$

In a small-amplitude wave, the wave height is small compared to the wavelength, so that  $k|h| \ll 1$  and  $e^{kh} \approx 1$  on the right hand side. Solving both equations for  $A$  we get

$$A = \frac{a\omega}{k} = \frac{ag_0}{\omega}. \quad (22-23)$$

Solving the last equality for  $\omega$  we obtain the dispersion law for deep-water waves

$$\boxed{\omega = \sqrt{g_0 k}}. \quad (22-24)$$

In terms of period and wavelength we have  $\tau = \sqrt{2\pi\lambda/g_0}$  which is of the same form as the previous estimate (22-6), except that now the numerical constant

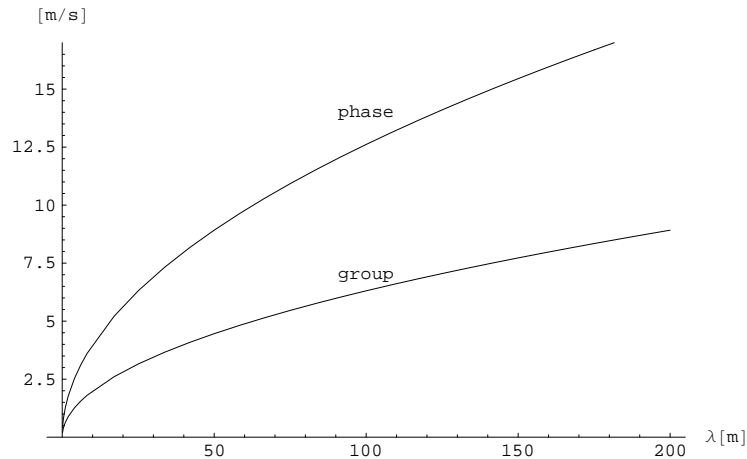


Figure 22.2: Phase and group velocities of deep-water waves as a function of wavelength. This figure corresponds to the small-wavelength part of fig. 22.3. Typical ocean swells have wavelengths of  $\lambda \approx 150$  m, phase velocity  $c \approx 15$  m/s  $\approx 55$  km/h and group velocity equal to half of this. Closer to the coast the waves slow down because the water gets shallower (see fig. 22.3).

has also been determined to be  $\sqrt{2\pi}$ . The corresponding deep-water phase and group velocities become

$$c = \sqrt{\frac{g_0}{k}} = \sqrt{\frac{g_0 \lambda}{2\pi}}, \quad c_g = \frac{1}{2}c. \quad (22-25)$$

and are plotted in fig. 22.2. Since the phase velocity is the double of the group velocity, the wave crests will move forward inside a wave packet.

The dispersive nature of deep-water waves have important consequences. A local surface disturbance in deep water — for example created by a storm far out at sea — usually contains more than one wavelength. The long-wave components are faster and will run ahead to arrive at the beach maybe a day or so before the slower short-wave components. The separation of wavelengths over long distances also causes the waves that arrive on the beach to be nearly monofrequent, rolling in at regular time intervals which slowly become shorter as the smaller wavelengths take over.

The complete deep-water solution for all the fields in the wave is,

$$\Psi = ace^{kz} \sin(kx - \omega t), \quad (22-26a)$$

$$v_x = awe^{kz} \cos(kx - \omega t), \quad (22-26b)$$

$$v_z = awe^{kz} \sin(kx - \omega t), \quad (22-26c)$$

$$p = p_0 - \rho_0 g_0 (z - ae^{kz} \cos(kx - \omega t)). \quad (22-26d)$$

The  $x$  and  $z$  velocities have the same scale,  $a\omega = 2\pi a/\tau$ , but are  $90^\circ$  out of phase. The fluid particles move through orbits that approximatively are circles of radius  $ae^{kz}$  at depth  $z$  (see problem 22.3).

Due to the exponential, a deep-water surface wave only influences the flow to a depth,  $|z| \approx 1/k = \lambda/2\pi$ , *i.e.* of the order one wavelength, as pointed out before. What happens at the bottom has no influence on the surface waves, as long as the ocean is much deeper than a wavelength.

### Harmonic line waves at finite depth

For a horizontally infinite container with perfectly flat impermeable bottom at constant depth  $z = -d$ , the only condition is that the vertical velocity should vanish at the bottom,

$$v_z = 0 \quad \text{for } z = -d. \quad (22-27)$$

In the absence of viscosity, we are not at liberty to impose a no-slip condition on the horizontal velocities.

If the depth is of the same magnitude as the wavelength, the bottom has influence on the flow, and the  $B$ -term in (22-22) becomes important. The flat-bottom boundary condition above implies that  $f'(-d) = 0$ , or  $Ae^{-kd} = Be^{kd}$ , so that we have

$$f(z) = C \cosh k(z + d) \quad (22-28)$$

where  $C$  is another constant. It is as for deep-water waves determined by the open surface boundary conditions (22-20), and we find for  $|h| \ll d$ ,

$$C = \frac{a\omega}{k \sinh kd} = \frac{ag_0}{\omega \cosh kd}. \quad (22-29)$$

The last equality yields the dispersion law,

$$\boxed{\omega = \sqrt{g_0 k \tanh kd}}, \quad (22-30)$$

with the corresponding phase and group velocities,

$$c = \sqrt{\frac{g_0}{k} \tanh kd}, \quad c_g = \frac{1}{2}c \left( 1 + \frac{2kd}{\sinh 2kd} \right). \quad (22-31)$$

They are plotted in fig. 22.3 for  $d = 20$  m. The phase velocity appears to curve downwards for all wavelengths, whereas the group velocity changes curvature twice, once for  $\lambda \approx 35$  m and once for  $\lambda \approx 70$  m. Generally, the finite depth becomes important from  $\lambda \gtrsim \pi d$ . For large wavelengths,  $kd \ll 1$  or  $\lambda \gg 2\pi d$ , both velocities approach the common value  $c = c_g = \sqrt{g_0 d}$ .

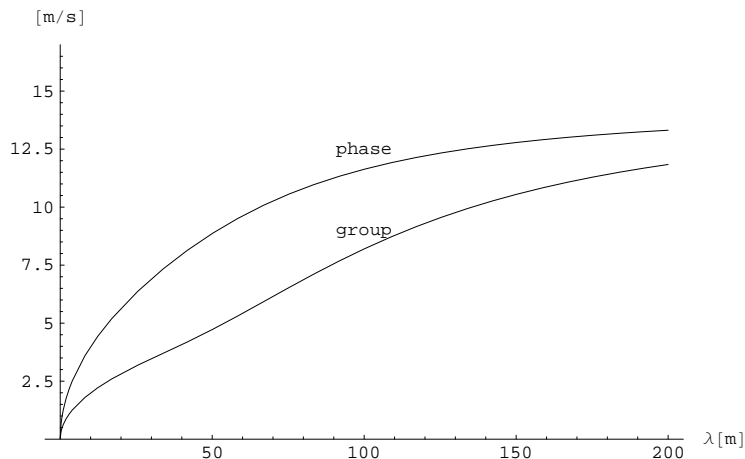


Figure 22.3: Phase and group velocities of flat-bottom gravity waves as a function of wavelength at a bottom depth of  $d = 20$  m. The phase and group velocities level out and become equal for large wavelengths, approaching the common shallow-water values of  $c = c_g = \sqrt{g_0 d} \approx 14$  m/s. The influence of the finite depth is clearly noticeable in the group velocity for  $\lambda \gtrsim \lambda_d \approx 63$  m.

The complete solution for all the fields underneath a small-amplitude harmonic line wave  $h = a \cos(kx - \omega t)$  at any depth  $d \gg a$  is finally,

$$\Psi = ac \frac{\cosh k(z+d)}{\sinh kd} \sin(kx - \omega t), \quad (22-32a)$$

$$v_x = a\omega \frac{\cosh k(z+d)}{\sinh kd} \cos(kx - \omega t), \quad (22-32b)$$

$$v_z = a\omega \frac{\sinh k(z+d)}{\sinh kd} \sin(kx - \omega t), \quad (22-32c)$$

$$p = p_0 - \rho_0 g_0 \left( z - a \frac{\cosh k(z+d)}{\cosh kd} \cos(kx - \omega t) \right). \quad (22-32d)$$

The pressure is clearly different from the purely hydrostatic pressure  $p_0 - \rho_0 g_0(z - h)$  of the water column above, although it oscillates in tune with the motion of the surface wave.

The fluid particle orbits are approximatively elliptical and become flatter as the bottom is approached, *i.e.* for  $z \rightarrow -d$  (problem 22.3). This implies that there is no net mass motion in the wave in the linear approximation (see however section 22.3). One might say that in the open sea, a passing small-amplitude wave leaves the water (roughly) where it found it.

### Shallow-water limit

For waves with wavelength much greater than the depth, *i.e.* for  $\lambda \gg 2\pi d$  or equivalently  $kd \ll 1$ , we have  $\tanh kd \approx kd$  and thus obtain the *shallow-water*

*dispersion law,*

$$\boxed{\omega = \sqrt{g_0 d} k} , \quad (22-33)$$

which confirms the correctness of the previous estimate (22-6). Shallow-water waves are non-dispersive with the same phase and group velocities

$$c = c_g = \sqrt{g_0 d} . \quad (22-34)$$

The leading terms in the solution become in the shallow wave limit,  $kd \ll 1$ ,

$$\Psi = \frac{ag_0}{\omega} \left( 1 + \frac{k^2(z+d)^2}{2} \right) \sin(kx - \omega t) , \quad (22-35a)$$

$$v_x \approx \frac{ca}{d} \cos(kx - \omega t) , \quad (22-35b)$$

$$v_z \approx a\omega \left( 1 + \frac{z}{d} \right) \sin(kx - \omega t) , \quad (22-35c)$$

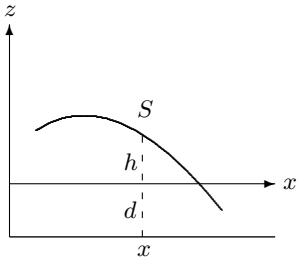
$$p \approx p_0 - \rho_0 g_0 (z - a \cos(kx - \omega t)) . \quad (22-35d)$$

The horizontal velocity is the same for all  $z$ , so that all the water underneath sloshes back and forth in unison as the wave proceeds. The vertical velocity decreases and reaches zero at the bottom, as it must (this the reason for keeping the second order terms in  $\Psi$ ). At any depth  $z$ , the pressure is just the hydrostatic pressure from the water column above, including the height of the wave. The horizontal velocity scale,  $ca/d = \lambda a/\tau d$ , equals precisely the previously estimated shallow-water value (22-3) which is larger than the vertical velocity scale  $2\pi a/\tau$  by a factor  $\lambda/2\pi d$ .

**Example 22.2.1 (Tsunami):** Huge shallow-water wave trains, tsunamis, with wavelengths up to 500 km can be generated by underwater earthquakes, landslides, volcanic eruptions, or large meteorite impacts. The average depth of the oceans is about 4000 m so tsunamis move with typical speeds of a passenger jet plane,  $c \approx 200 \text{ m/s} \approx 720 \text{ km/h}$ , in deep waters. For  $\lambda = 500 \text{ km}$  the period becomes  $\tau = \lambda/c \approx 2500 \text{ s} \approx 42 \text{ minutes}$ , but since the amplitude is small, say  $a \approx 1 \text{ m}$ , a tsunami will be completely imperceptible for a ship at sea. When the tsunami approaches a coastline, the water depth decreases and the wave slows down while increasing its amplitude with sometimes devastating effect on the shore.

## 22.3 Wave energy and momentum

Waves contain mass, momentum, and energy, and the movement of fluid also moves these quantities around. Although there is no net transport of mass, momentum, or energy in a gravity wave to first order in the amplitude  $a$ , we shall see that there will in fact be in second order.



A vertical cut  $S$  through the wave (dashed). Its length is  $L$  in the  $y$ -direction.

### Mass transport

The rate of mass transported through a vertical cut  $S$  through the wave of length  $L$  in the  $y$ -direction is

$$Q = \int_S \rho_0 \mathbf{v} \cdot d\mathbf{S} = \int_{-d}^h \rho_0 v_x L dz . \quad (22-36)$$

Under the small-amplitude assumption,  $|h| \ll d$ , we can expand the integral to first order in  $h$  to get<sup>1</sup>,

$$Q = \rho_0 L \int_{-d}^0 v_x dz + \rho_0 L h v_x|_{z=0} . \quad (22-37)$$

The first term oscillates in tune with the wave and represents the amount of water that is merely sloshing back and forth. Inserting (22-32b) this term is seen to be of the form  $Q_0 \cos(kx - \omega t)$  with amplitude

$$Q_0 = \rho_0 L a c . \quad (22-38)$$

What we are really interested in is the average mass transport during a complete period,

$$\langle Q \rangle = \frac{1}{\tau} \int_0^\tau Q dt . \quad (22-39)$$

Since  $\langle v_x \rangle = 0$  the first (sloshing) term in  $Q$  gives no contribution, so that we get

$$\frac{\langle Q \rangle}{\rho_0 L} = \langle h v_x|_{z=0} \rangle = a^2 \omega \coth kd \langle \cos^2(kx - \omega t) \rangle = \frac{1}{2} a^2 \omega \coth kd .$$

In the last step have used that the average of the squared cosine over a complete period is  $1/2$ . Finally, simplifying by means of the dispersion law (22-30) we arrive at

$$\langle Q \rangle = \frac{\rho_0 g_0 L a^2}{2c} , \quad (22-40)$$

where  $c = \omega/k$  is the phase velocity. Somewhat against intuition, the mass flow is smaller the higher the phase velocity. The ratio between the sloshing amplitude and the average mass flow is,

$$\frac{\langle Q \rangle}{Q_0} = \frac{g_0 a}{2c^2} , \quad (22-41)$$

which is indeed small for small-amplitude waves.

**Example 22.3.1:** A wave with  $a = 0.1$  m and phase velocity  $c = 10$  m/s, transports on the average  $\langle Q \rangle / L = 5$  kg/s/m per unit of transverse length. A destructive tsunami with  $a = 1$  m and  $c = 200$  m/s only carries an average mass flow of  $\langle Q \rangle / L = 25$  kg/s/m.

<sup>1</sup>There is a subtlety in this expression because there could be corrections of order  $h$  to the field  $v_x$  (see problem 22.7).

### Total energy

Consider a thin column of water of width  $\Delta x$  along  $x$  and length  $L$  along  $y$ , so that its “footprint” area is  $A = \Delta x L$ . Relative to the static water level  $z = 0$ , its potential energy is,

$$\mathcal{V} = \int_V \rho_0 g_0 z dV = \int_0^h \rho_0 g_0 z A dz = \frac{1}{2} \rho_0 g_0 h^2 A, \quad (22-42)$$

The potential energy is always positive, and rises and falls in tune with the square of the wave height  $h = a \cos(kx - \omega t)$ . Its time average over a full period  $\tau$  becomes

$$\langle \mathcal{V} \rangle = \frac{1}{2} \rho_0 g_0 \langle h^2 \rangle A = \frac{1}{4} \rho_0 g_0 a^2 A. \quad (22-43)$$

This result agrees in magnitude with the estimate on page 416 for  $A = \lambda^2$ .

The kinetic energy of the water in the column is similarly

$$\mathcal{T} = \int_V \frac{1}{2} \rho_0 \mathbf{v}^2 dV = \int_{-d}^h \frac{1}{2} \rho_0 (v_x^2 + v_z^2) A dz \approx \int_{-d}^0 \frac{1}{2} \rho_0 (v_x^2 + v_z^2) A dz. \quad (22-44)$$

In the last step we have used that the amplitude is small,  $|h| \ll d$ , and replaced  $h$  by 0 in the upper limit of the integral. Inserting the explicit gravity wave solution (22-32), we obtain the time average of the integrand,

$$\langle v_x^2 + v_z^2 \rangle = \frac{1}{2} \left( \frac{a\omega}{\sinh kd} \right)^2 (\cosh^2 k(z+d) + \sinh^2 k(z+d)).$$

Finally, making use of the relation  $\cosh^2 \phi + \sinh^2 \phi = \cosh 2\phi$ , the integral over  $z$  can be done, and we find after some rearrangement,

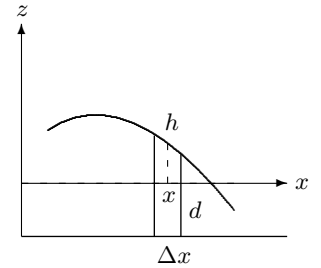
$$\langle \mathcal{T} \rangle = \frac{1}{4} \rho_0 A \left( \frac{a\omega}{\sinh kd} \right)^2 \frac{\sinh 2kd}{2k} = \frac{1}{4} \rho_0 g_0 a^2 A. \quad (22-45)$$

As expected, we have  $\langle \mathcal{T} \rangle = \langle \mathcal{V} \rangle$  (see also problem 22.10). The average of the total energy thus becomes

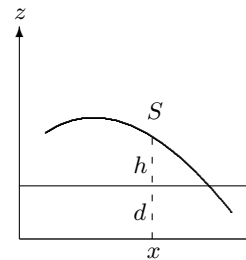
$$\boxed{\langle \mathcal{E} \rangle = \langle \mathcal{T} \rangle + \langle \mathcal{V} \rangle = \frac{1}{2} \rho_0 g_0 a^2 A,} \quad (22-46)$$

Somewhat surprisingly, the average energy per unit of surface area,  $\langle \mathcal{E} \rangle / A$ , only depends on the amplitude and not on the depth or wavelength.

**Example 22.3.2:** A small-amplitude surface wave in water with amplitude  $a = 1$  m thus carries an energy of about  $\langle \mathcal{E} \rangle / A = 5000$  J/m<sup>2</sup>.



A thin water column of “footprint” area  $A = \Delta x L$  and height  $h$  in a sea of depth  $d$ .



A vertical cut  $S$  through wave (dashed). Its length  $L$  in the  $y$ -direction.

### Wave power

Waves are able to do work and many ingenious schemes have been thought up for the exploitation of wave power. The power of a wave may be calculated from the rate of work performed by the pressure on a vertical cut  $S$  through the wave,

$$P = \int_S p \mathbf{v} \cdot d\mathbf{S} = \int_{-d}^h p v_x L dz \approx \int_{-d}^0 p v_x L dz . \quad (22-47)$$

Writing the pressure (22-32d) as  $p = p_0 - \rho_0 g_0 z + \rho_0 c v_x$  and using that  $\langle v_x \rangle = 0$ , we find the average  $\langle p v_x \rangle = \rho_0 c \langle v_x^2 \rangle$ . Inserting  $v_x$  from (22-32b) we find,

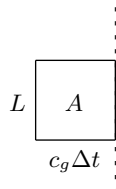
$$\langle v_x^2 \rangle = \frac{1}{2} \left( \frac{a\omega}{\sinh kd} \right)^2 \cosh^2 k(z+d) .$$

Finally, using that  $2 \cosh^2 \phi = 1 + \cosh 2\phi$  the integral can be done, and the average power of the wave may be written

$$\langle P \rangle = \frac{1}{4} \rho_0 g_0 a^2 c \left( 1 + \frac{2kd}{\sinh 2kd} \right) = \frac{1}{2} \rho_0 g_0 a^2 L c_g , \quad (22-48)$$

where the group velocity is given by (22-31).

We can now confirm the claim that energy indeed moves with the group velocity even if the wave contains only one wave number, because we have  $\langle E \rangle = \langle P \rangle \Delta t$  where  $\Delta t = \Delta x / c_g$  is the time it takes for a group of waves to move through the distance  $\Delta x$ , covering an area  $A = L \Delta x$ .



The energy contained in the rectangle  $A = L \times \Delta x$  passes the dashed line in the time  $\Delta t = \Delta x / c_g$ .

**Example 22.3.3:** The tsunami of example 22.2.1 with  $\lambda = 500$  km,  $c_g = 200$  m/s, and  $a = 1$  m carries an average power per unit of transverse length of  $\langle P \rangle / L = 10^6$  W/m. Such a Tsunami can really wreak havoc when it hits a coast.

### Wave force from momentum transport

The total momentum transport through the vertical cut may be taken as a measure of the force that the moving fluid exerts in the cut,

$$\mathcal{F}_x = \int_S \rho_0 v_x \mathbf{v} \cdot d\mathbf{S} = \int_{-d}^h \rho_0 v_x^2 L dz \approx \int_{-d}^0 \rho_0 v_x^2 L dz . \quad (22-49)$$

There is a small subtlety in using the relation between momentum transport and force which is cleared up in problem 22.8. Averaging over time and using  $\langle v_x^2 \rangle$  from above we find

$$\langle \mathcal{F}_x \rangle = \frac{\langle P \rangle}{c} = \frac{1}{2} \rho_0 g_0 a^2 L \frac{c_g}{c} . \quad (22-50)$$

This is related to the force of a wave hitting an obstacle, although that is strongly complicated by the shape of the obstacle and by reflected waves [60].

**Example 22.3.4:** If you are  $L = 50$  cm wide and wade near the shore, a wave of amplitude  $a = 10$  cm would act on you with an average force of  $\langle \mathcal{F}_x \rangle \approx \frac{1}{2} \rho_0 g_0 L a^2 = 25$  N. That won't topple you.

### Rise of a shallow-water swell

When a small-amplitude wave train with wavelength much larger than the depth approaches a gently sloping beach, the phase and group velocity of the waves will fall with decreasing water depth according to the shallow-water expression (22-34). It is well-known that the amplitude grows at the same time, but how fast does it grow? And what about the wavelength?

Suppose the waves roll steadily in from afar with constant period  $\tau$ . In the steady situation, wave crests cannot accumulate anywhere, so that the same number of waves must hit the coast in a given time interval as roll in from far away, implying that the period  $\tau$  between successive wave crests must be the same everywhere, independently of the bottom depth. The constancy of  $\tau$  in turn implies that the wavelength must scale with depth like the phase velocity,  $\lambda = c\tau \sim \sqrt{d}$ . Similarly, energy cannot accumulate anywhere in the steady situation, so that the average rate of energy transport  $\langle P \rangle \sim a^2 c_g \sim a^2 \sqrt{d}$  must be independent of  $d$ , implying that  $a \sim d^{-1/4}$ . Altogether, these considerations show that a shallow-water wave starting out at depth  $d_0$  with amplitude  $a_0$  and wavelength  $\lambda_0$ , will have

$$a = a_0 \left( \frac{d_0}{d} \right)^{1/4}, \quad \lambda = \lambda_0 \sqrt{\frac{d}{d_0}}, \quad (22-51)$$

when the depth is reduced to  $d$  (see fig. 22.4).

These expressions are only valid for very gently sloping beaches which may be viewed as locally flat so that the waves propagate according to the shallow-water expressions everywhere. When this is not fulfilled, the bottom boundary condition must take into account the actual beach slope  $d'(x)$ , and a much more complicated formalism ensues [59]. On top of that, there are the unavoidable non-linear effects close to the shore where the depth becomes comparable to the amplitude.

**Example 22.3.5 (Ocean swell):** Typical wind-generated oceanic swells have wavelengths of  $\lambda_0 = 150$  m, velocity  $c_0 = 15$  m/s, period  $\tau = 10$  s in deep water, and perhaps an amplitude of  $a_0 = 1$  m. When the depth decreases to about  $d_0 \approx \lambda_0/2\pi \approx 25$  m, the water becomes shallow and the wave starts to rise. At a depth of  $d \approx 2$  m, the wave characteristics are  $a \approx 2$  m,  $\lambda \approx 43$  m,  $c = 4.5$  m/s. At this point, the amplitude has become equal to the depth and strong non-linear effects will take over the wave, so that it breaks and produces a surf.



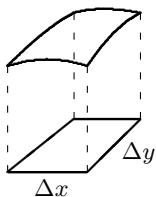
Figure 22.4: Gravity waves coming in from the right towards a coast along a gently sloping flat bottom. The waves increase gently in amplitude as they decrease in wave-length. When the amplitude becomes comparable to the depth (on the left), non-linear effects take over and make the waves break.

**Example 22.3.6 (Tsunami):** A tsunami with  $\lambda_0 = 500$  km,  $\tau = 2500$  s,  $a_0 = 1$  m,  $c_0 = 200$  m/s at a water depth  $d_0 = 4000$  m rises to  $a = 4.5$  m,  $\lambda = 25$  km, and  $c = 10$  m/s at a depth of  $d = 10$  m. Beyond this point non-linear effects set in and the tsunami will break. At the coast this tsunami appears as a sequence of powerful tidal waves arriving every 42 minutes and rolling far inland.

## 22.4 Capillary surface waves

Surface tension was introduced in section 8.1 on page 126 and was shown to exert strong influence on the shapes small fluid objects at rest, for example raindrops. In this section we shall study the interplay between gravity and surface tension for surface waves.

Surface tension is characterized by a material constant  $\alpha$ , representing the attractive force per unit of length of the surface, or equivalently the extra energy per unit of surface area from the missing molecular bonds. Surface tension generates a pressure jump (8-5) across any interface between two fluids, expressed through the principal radii of curvature of the surface. We saw in section 8.1 that the relative influence of surface tension and gravity in a liquid/air interface is characterized by a characteristic length (8-4), called the *capillary constant* or the *capillary radius*, which is  $R_c = \sqrt{\alpha/\rho_0 g_0} \approx 2.7$  mm for the interface between water and air. Surface tension only plays a major role for length scales around and below the capillary constant.



The small rectangle in the  $xy$ -plane defines a piece of the wave surface of area  $A = \Delta x \Delta y$ .

### Pressure jump across a nearly flat surface

To calculate the pressure jump over a nearly flat surface,  $z = h(x, y)$  with  $|\partial h/\partial x|, |\partial h/\partial y| \ll 1$ , we consider a tiny piece of the surface situated above a small rectangle between  $(x, y)$  and  $(x + \Delta x, y + \Delta y)$ . All four sides of this piece of surface are subject to tension from the surroundings, and we wish to calculate the resultant vertical force. Since the slope of the surface is small, we may disregard the slight misalignment between the vertical force and the pressure force which strictly speaking must be orthogonal to the surface. The slope of the surface at  $(x, y)$  is  $\partial h/\partial x$  along  $x$ , and it follows from the geometry that the surface

tension acting on the two  $\Delta y$ -sides of the rectangle generates a vertical force

$$\Delta \mathcal{F}_z = -\alpha \Delta y \frac{\partial h(x, y)}{\partial x} + \alpha \Delta y \frac{\partial h(x + \Delta x, y)}{\partial x} \approx \alpha \Delta x \Delta y \frac{\partial^2 h(x, y)}{\partial x^2} .$$

Adding the forces acting on the two  $\Delta x$ -sides and dividing by the area  $A = \Delta x \Delta y$ , we see that in order to balance the vertical force from surface tension, the pressure just below the surface must be higher by,

$$\Delta p = -\alpha (\nabla_x^2 + \nabla_y^2) h . \quad (22-52)$$

If the surface curves downwards in all directions in a given point, we have  $(\nabla_x^2 + \nabla_y^2)h < 0$ , and the extra pressure will be positive below the surface.

The curvature of a small-amplitude surface wave thus generates a pressure jump  $\Delta p$  at the surface. Whereas the Euler equation (22-15) is unchanged, the value of the pressure just below the surface is  $p_0 + \Delta p$  rather than  $p_0$ , so that the dynamic boundary condition (22-17) is replaced by,

$$p = p_0 + \Delta p \quad \text{for } z = h . \quad (22-53)$$

Since  $\Delta p$  given by (22-52) is positive at a wave crest and negative at a trough, surface tension collaborates with gravity in attempting to flatten the water surface. Waves completely dominated by surface tension are called *capillary waves*.

### Deep-water capillary gravity waves

Surface tension is only expected to become important for waves of very small wavelength, which except for special situations may be assumed to be deep-water waves. The velocity potential is in that case  $\Psi = Ae^{kz} \sin(kx - \omega t)$ , and from the kinematic boundary condition (22-16) and the modified dynamic boundary condition (22-53) we obtain in the usual way,

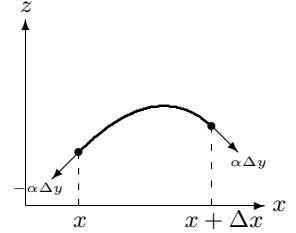
$$A = a \frac{\omega}{k} = a \frac{\rho_0 g_0 + \alpha k^2}{\rho_0 \omega} . \quad (22-54)$$

This shows that the only effect of surface tension is to increase the gravitational acceleration from  $g_0$  to,

$$g = g_0 + \frac{\alpha k^2}{\rho_0} = g_0 (1 + k^2 R_c^2) , \quad (22-55)$$

where we have introduced the capillary constant  $R_c = \sqrt{\alpha / \rho_0 g_0}$ . As foreseen, surface tension collaborates with gravity and becomes more important than gravity for  $kR_c \gtrsim 1$ , or

$$\lambda \lesssim \lambda_c = 2\pi R_c . \quad (22-56)$$



The total vertical force on the small piece of surface is determined by projecting the forces due to surface tension on the vertical.

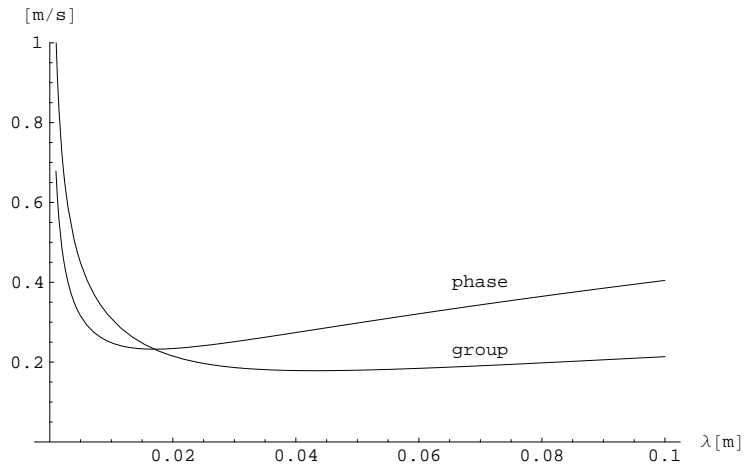


Figure 22.5: Phase and group velocities for deep-water capillary gravity waves (in water) as a function of the wavelength  $\lambda = 2\pi/k$ . For  $\lambda \lesssim 5$  cm surface tension makes phase and group velocities rise again. Phase and group velocities cross each other at  $\lambda = \lambda_c = 1.7$  cm.

In water this capillary wavelength is  $\lambda_c \approx 1.7$  cm.

Replacing  $g_0$  by  $g$  in the deep-water dispersion law (22-24), we find

$$\omega = \sqrt{g_0 k + \frac{\alpha}{\rho_0} k^3} = \sqrt{g_0 k (1 + k^2 R_c^2)}. \quad (22-57)$$

This dispersion law agrees very well with experiments (see for example Christiansen et al, J. Fluid Mech. **291**, 323 (1995)).

The phase and group velocities

$$c = \sqrt{\frac{g_0}{k} (1 + k^2 R_c^2)}, \quad c_g = \frac{1}{2} c \frac{1 + 3k^2 R_c^2}{1 + k^2 R_c^2}. \quad (22-58)$$

are plotted for water in fig. 22.5. Notice that the phase velocity has a minimum for  $kR_c = 1$  (i.e.  $\lambda = \lambda_c$ ) where the group velocity also equals the phase velocity (see problem 22.13). The minimum of the group velocity occurs for a somewhat larger wavelength.

For very small wavelengths,  $\lambda \ll \lambda_c$  or  $kR_c \gg 1$ , surface tension dominates completely, and we find the dispersion law for purely capillary waves,

$$\omega = \sqrt{\frac{\alpha k^3}{\rho_0}}, \quad c = \sqrt{\frac{\alpha k}{\rho_0}}, \quad c_g = \frac{3}{2} c. \quad (22-59)$$

In purely capillary waves the phase velocity is only 2/3 of the group velocity, and the wave crests appear to move backwards inside a wave packet!

## 22.5 Internal waves

In the ocean a heavier saline layer of water may often be found below a lighter more brackish layer, and so-called *internal waves* may arise in the interface. Even if the difference in density between the fluids is small, the equilibrium interface will always be horizontal with the lighter liquid situated above the heavier, as discussed previously in section 7.1. Were it somehow possible to invert the ocean so that the lighter fluid came to lie below the heavier, instability would surely arise, and the liquids would after some time find back to their “natural” order. As we shall see, surface tension can in fact stabilize the inverted situation in sufficiently small containers.

### Boundary conditions

Let the lower layer have density  $\rho_1$  and the upper layer  $\rho_2$  with a separating interface  $z = h(x, y, t)$  between the two fluids with velocity potentials  $\Psi_1$  and  $\Psi_2$ . For small-amplitude waves, the kinematic boundary conditions express that both fluids and the separating surface must move together in the vertical direction,

$$v_{1z} = v_{2z} = \frac{\partial h}{\partial t} \quad \text{for } z = h. \quad (22-60)$$

Including surface tension (22-52), the dynamic boundary condition becomes,

$$p_1 + \Delta p = p_2 \quad \text{for } z = h. \quad (22-61)$$

where  $\Delta p$  is given by (22-52), and the pressures are expressed like (22-19) in each of the fluids.

### Dispersion law

Suppose again that the interface takes the form of a pure line wave,  $h = a \cos(kx - \omega t)$ . We shall only consider deep-water waves in which the wave flow is required to vanish far below and far above the interface. The velocity potentials are then of the same form as for deep-water waves,

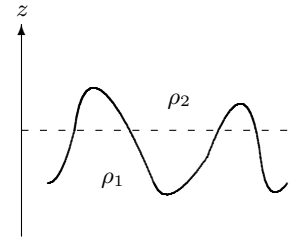
$$\Psi_1 = A_1 e^{+kz} \sin(kx - \omega t), \quad \Psi_2 = A_2 e^{-kz} \sin(kx - \omega t),$$

with a notable change of sign in the exponential factors. The boundary conditions (22-60) and (22-61) imply for  $k|h| \ll 1$  that

$$kA_1 = -kA_2 = a\omega, \quad \rho_1(g_0 a - \omega A_1) + \alpha k^2 a = \rho_2(g_0 a - \omega A_2). \quad (22-62)$$

Solving these we find,

$$A_1 = -A_2 = \frac{a}{\omega} \frac{g_0(\rho_1 - \rho_2) + \alpha k^2}{\rho_1 + \rho_2} = a \frac{\omega}{k}. \quad (22-63)$$



*Internal waves at an interface with a heavier liquid below and a lighter above.*

From the last equality we obtain the *dispersion law for deep-water internal waves*,

$$\omega = \sqrt{\frac{g_0 k (\rho_1 - \rho_2) + \alpha k^3}{\rho_1 + \rho_2}}. \quad (22-64)$$

If the upper density is much smaller than the lower,  $\rho_2 \ll \rho_1$ , these waves become ordinary deep-water gravity waves, but when the densities are nearly equal,  $\rho_2 \lesssim \rho_1$ , the internal waves have much lower frequencies (and velocities) than waves of the same wavelength at the surface. The capillary constant is as before defined as the length scale where gravity and surface tension are of the same magnitude,

$$R_c = \sqrt{\frac{\alpha}{|\rho_1 - \rho_2| g_0}}. \quad (22-65)$$

It diverges when the densities become equal, because gravity then plays no role, and internal waves become purely capillary waves.

**Example 22.5.1:** If a brackish surface layer lies above a saline layer with 4% higher density, the capillary wavelength for internal waves becomes  $\lambda_c = 2\pi R_c = 2.7$  m. A wave of this wavelength has period  $\tau = 6.6$  s, and moves with the majestic speed of  $c = 0.4$  m/s.

### The Rayleigh-Taylor instability

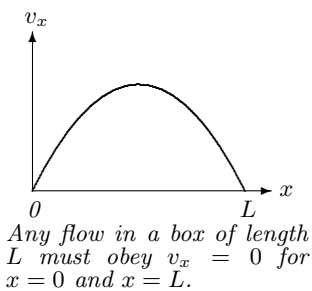
When the heavier fluid lies below the lighter,  $\rho_1 > \rho_2$ , the frequency  $\omega$  of an internal wave is always real, but if the container is quickly turned upside down, such that  $\rho_1 < \rho_2$ , the heavier fluid will be on top, and the dispersion law may be written as,

$$\omega = \sqrt{g_0 \frac{\rho_2 - \rho_1}{\rho_1 + \rho_2} k (k^2 R_c^2 - 1)}, \quad (22-66)$$

The argument of the squareroot will be negative for  $kR_c < 1$ , or  $\lambda > \lambda_c = 2\pi R_c$ . In that case,  $\omega$  becomes imaginary, and the otherwise sinusoidal form the line wave is replaced by an exponential growth  $e^{|\omega|t}$  in time. This signals an instability, called the *Rayleigh-Taylor instability*.

In an infinitely extended ocean, there is room for waves with wavelengths of any size, and the inverted situation will always be unstable. It can only be maintained for a very short while, because the smallest perturbation of the surface will lead to a run-away process that ends with the heavier liquid again being arranged below the lighter.

In a finite container, there is an upper limit to the allowed wavelengths, because the boundary conditions require the horizontal velocities to vanish at the vertical walls surrounding the fluids. Any flow in a finite box-shaped container of horizontal length  $L$  must obey the boundary conditions  $v_x = 0$  for both  $x = 0$  and  $x = L$ . Linear Euler flow in a box can, like the flows we are studying here,



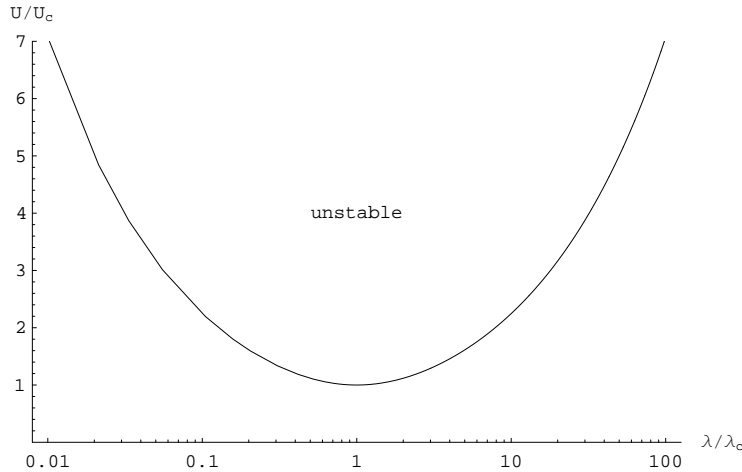


Figure 22.6: Plot of  $U/U_c$  as a function of  $\lambda/\lambda_c$ . For the water-air interface the capillary wavelength is  $\lambda_c = 1.7$  cm and the critical velocity is  $U_c = 7.4$  m/s. For a given velocity  $U$ , one can read off the range of unstable wavelengths from this figure.

always be resolved into a superposition of standing waves with horizontal velocity  $v_x \sim \sin kx \cos \omega t$ . The boundary conditions select the allowed wave numbers to be  $k = n\pi/L$  where  $n = 1, 2, \dots$  is an arbitrary integer. For  $n = 1$  we obtain the largest wavelength,  $\lambda = 2\pi/k = 2L$ , and this shows as long as

$$L < \frac{1}{2}\lambda_c = \pi R_c = \pi \sqrt{\frac{\alpha}{(\rho_2 - \rho_1)g_0}}, \quad (22-67)$$

unstable wave modes with  $\lambda > \lambda_c$  cannot occur. If a container with horizontal size smaller than half the capillary wavelength is inverted, the heavier liquid will remain stably on top of the lighter.

**Example 22.5.2:** Air against water has as we have seen before a capillary wavelength of  $\lambda_c = 1.7$  cm so that we must require  $L < 0.85$  cm. Try it yourself with a glass tube of, for example, 5 mm diameter. It works!

### The Kelvin-Helmholtz instability

Layers of inviscid fluids are capable of sliding past each other with a finite slip-velocity, if we disregard the viscous boundary layers that otherwise will soften the sharp discontinuity in velocity. When waves arise in the interface between the fluids, they will so to speak “get in the way” of the smooth flow, leading us to expect instability at a sufficiently high slip-velocity.

Suppose the upper layer is moving with velocity  $U$  in the restframe of the lower layer. Taking into account the slope  $\nabla_x h$  of the interface, the horizontal flow in the upper layer will add  $U\nabla_x h$  to the vertical velocity, such that the

kinematic boundary conditions are replaced by,

$$v_{1z} = \frac{\partial h}{\partial t}, \quad v_{2z} = \frac{\partial h}{\partial t} + U \nabla_x h \quad \text{for } z = h. \quad (22-68)$$

The same is the case for the pressure which becomes

$$p_2 = p_0 - \rho_0 \left( g_0 h + \frac{\partial \Psi_2}{\partial t} + U \nabla_x \Psi_2 \right). \quad (22-69)$$

Putting it all together we find the boundary conditions,

$$\begin{aligned} kA_1 &= a\omega, & -kA_2 &= a(\omega - kU), \\ \rho_1(g_0 a - \omega A_1) + \alpha k^2 a &= \rho_2(g_0 a - (\omega - kU)A_2), \end{aligned}$$

which when combined lead to a quadratic equation for the frequency

$$(\rho_1 + \rho_2)\omega^2 - 2\rho_2 k U \omega + \rho_2 k^2 U^2 = k((\rho_1 - \rho_2)g_0 + \alpha k^2). \quad (22-70)$$

Given the wave number  $k$ , the roots are real for

$$U^2 < \left( \frac{1}{\rho_1} + \frac{1}{\rho_2} \right) \frac{(\rho_1 - \rho_2)g_0 + \alpha k^2}{k}. \quad (22-71)$$

For  $\rho_1 > \rho_2$ , the right hand side has an absolute minimum when  $kR_c = 1$ , where  $R_c$  is the capillary radius for internal waves (22-65). Selecting the minimum of the right hand side by setting  $k = 1/R_c$ , the condition for absolute stability becomes

$$U < U_c = \sqrt{2g_0 R_c \left( \frac{\rho_1}{\rho_2} - \frac{\rho_2}{\rho_1} \right)}. \quad (22-72)$$

For air flowing over water the critical velocity is  $U_c = 7.4$  m/s. In fig. 22.6 the ratio

$$\frac{U}{U_c} = \sqrt{\frac{1}{2} \left( \frac{\lambda}{\lambda_c} + \frac{\lambda_c}{\lambda} \right)} \quad (22-73)$$

is plotted as a function of  $\lambda/\lambda_c$ . For  $U > U_c$  there will be a range of wavelengths around the capillary wavelength  $\lambda = \lambda_c$  for which small disturbances will diverge exponentially with time. This is the *Kelvin-Helmholtz* instability which permits us at least in principle to understand how the steadily streaming wind is able to generate waves from infinitesimal disturbances.

What actually happens to the unstable waves with their exponentially growing amplitudes, for example how they grow into the larger waves created by a storm, cannot be predicted from linear theory. It is, however, possible to say something about the statistics of wind-generated ocean waves without going into too much nonlinear theory (see section 22.7).

## \* 22.6 Attenuation of small-amplitude waves

Surface waves are attenuated by several effects. First of all, there is viscous attenuation due to internal friction in the fluid. Secondly, there is attenuation from bottom friction, and thirdly there is dissipation due to deviations of surface tension from its equilibrium value, which for example plays a role when oil is poured on troubled waters. Here we shall only focus on viscous attenuation.

### Rate of viscous dissipation

In an incompressible liquid, we have  $\nabla \cdot \mathbf{v} = 0$ , and the internal rate of viscous energy dissipation (17-79) in a thin vertical column of liquid with area  $A$  simplifies to

$$P_{\text{int}} = -2\eta \int_{-d}^h \sum_{ij} v_{ij}^2 A dz \approx -2\eta \int_{-d}^0 \sum_{ij} v_{ij}^2 A dz, \quad (22-74)$$

where  $v_{ij} = \frac{1}{2}(\nabla_i v_j + \nabla_j v_i)$  and  $\eta$  is the viscosity. For a line wave running along  $x$  the integrand may be recast as

$$\sum_{ij} v_{ij}^2 = (\nabla_x v_x)^2 + (\nabla_z v_z)^2 + \frac{1}{2}(\nabla_x v_z + \nabla_z v_x)^2 = 2(\nabla_x v_x)^2 + 2(\nabla_x v_z)^2.$$

In the last step have used mass conservation  $\nabla_z v_z = -\nabla_x v_x$  and irrotationality  $\nabla_z v_x = \nabla_x v_z$ . For a harmonic wave (22-32) we may replace  $\nabla_x$  by  $k$  in the time average, so that it becomes

$$\left\langle \sum_{ij} v_{ij}^2 \right\rangle = 2k^2 \langle v_x^2 + v_z^2 \rangle. \quad (22-75)$$

This is proportional to the integrand in the kinetic energy (22-44) and taking over the result (22-45) this leads to  $\langle -P_{\text{int}} \rangle = 8\nu k^2 \langle T \rangle$ , where  $\nu = \eta/\rho_0$  is the kinematic viscosity. Relative to the average of the total energy,  $\langle \mathcal{E} \rangle = 2 \langle T \rangle$  the rate of dissipation finally becomes

$$\boxed{\frac{\langle -P_{\text{int}} \rangle}{\langle \mathcal{E} \rangle} = 4\nu k^2.} \quad (22-76)$$

The dissipative energy loss grows quadratically with the wave number and is most important for small wavelengths, *i.e.* for capillary waves. These may as before be included by replacing  $g_0$  by the effective gravity (22-55), but that does not change the above result.

The loss of energy over a wave period  $\tau = 2\pi/\omega$  is  $P_{\text{int}} \tau$ , and relative to the average energy of the wave (22-46), it becomes

$$\frac{\langle -P_{\text{int}} \rangle \tau}{\langle \mathcal{E} \rangle} = 4\nu k^2 \tau = 8\pi\nu \frac{k^2}{\omega} = 16\pi^2 \frac{\nu\tau}{\lambda^2}, \quad (22-77)$$

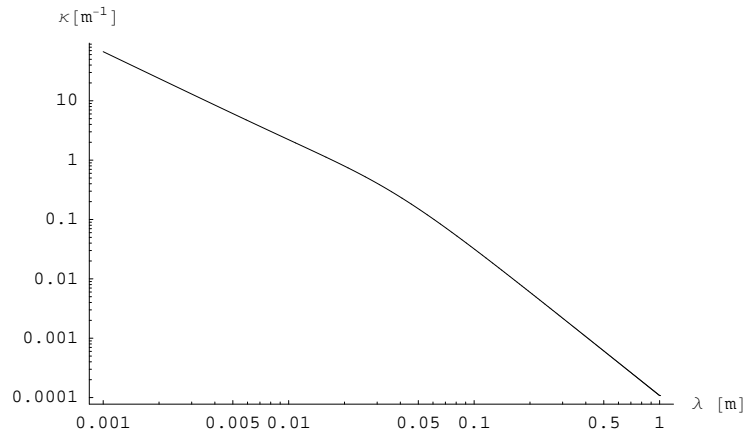


Figure 22.7: The viscous amplitude attenuation coefficient  $\kappa$  for water plotted as a function of wavelength  $\lambda$ . The viscosity is  $\nu = 8.64 \times 10^{-7} \text{ m}^2/\text{s}$  and the surface tension  $\alpha = 0.073 \text{ N/m}$ . Viscous attenuation essentially only plays a role for very small wavelengths.

where  $\nu$  is the kinematic viscosity. The condition for our calculation to be valid is that the relative attenuation should be small. In deep water with  $\nu \approx 10^{-6} \text{ m}^2/\text{s}$ , this quantity becomes larger than unity for  $\lambda \lesssim 40 \text{ }\mu\text{m}$ , so that the condition should be well satisfied in practice where wavelengths are much larger.

### Energy and amplitude attenuation coefficients

The energy propagates, as we have shown before, with the group velocity  $c_g$ . Dividing the rate of dissipation (22-76) by  $c_g$ , we obtain the spatial *energy attenuation coefficient* (i.e. the relative loss of energy per unit of length)

$$2\kappa = \frac{4\nu k^2}{c_g}. \quad (22-78)$$

As the energy is quadratic in the amplitude, the energy attenuation coefficient is twice the *amplitude attenuation coefficient*  $\kappa$ , plotted in fig. 22.7. It is clearly only of importance for small wavelengths.

**Example 22.6.1:** In water for  $\lambda = 1 \text{ m}$  one finds  $\kappa \approx 10^{-4} \text{ m}^{-1}$  whereas for  $\lambda = \lambda_c = 1.7 \text{ cm}$  one gets  $\kappa \approx 1 \text{ m}^{-1}$ . A raindrop hitting a lake surface thus creates a disturbance that dies out after propagating through a meter or less whereas a big object, like the human body, will make waves with longer wavelength that continue essentially unattenuated right across the lake. In these cases, however, the amplitude of the ring-shaped surface waves will also diminish for purely geometric reasons.

## \* 22.7 Statistics of wind-generated ocean waves

Waves arise spontaneously from tiny perturbations at the wind/water interface when the wind speed surpasses the Kelvin-Helmholtz instability threshold (see page 435). The continued action of the wind and nonlinear wave interactions raise the waves further, until a kind of dynamic equilibrium is reached in which the surface may be viewed as a statistical ensemble of harmonic waves with a spectrum of periods, wavelengths, and amplitudes. Even if we do not understand the mechanism at play, it is nevertheless possible to draw some general conclusions about its statistics and compare them with observations.

### Surface height observations

A ship or buoy bobbing at a fixed position  $(x, y)$  of the ocean surface reflects the local surface height,  $h(t) = h(x, y, t)$ . The variations in surface height may be determined by many different techniques, for example based on accelerometers, radar or satellites. While the wind blows steadily, a long record of  $N \gg 1$  measurements  $h_n = h(t_n)$  can be collected at the discrete times,  $t_n = n\epsilon$  ( $n = 1, 2, \dots, N$ ), which for simplicity are assumed to be evenly spaced.

The underlying wave structure of the surface creates strong correlations between successive measurements of the local height. Short waves are carried on top of larger waves and so on. To get rid of such correlations, we shall for odd  $N = 2M + 1$  write the record as a superposition of simple harmonics (see problem 22.15 for the precise theory of discrete Fourier transformations),

$$h_n = a_0 + \sum_{m=1}^M a_m \cos(\omega_m t_n - \chi_m) \quad (22-79)$$

where  $\omega_m = 2\pi m/N\epsilon$  is the circular frequency,  $a_m$  the amplitude, and  $\chi_m$  the phase shift of the  $m$ 'th harmonic. Given the  $N = 2M + 1$  measured values  $h_n$  these equations may be solved for the  $2M + 1$  unknowns, consisting of amplitudes and phase shifts plus the constant  $a_0$ . Notice that the highest frequency that can be resolved by  $N$  observations is  $\omega_M = 2\pi M/N\epsilon \approx \pi/\epsilon$ .

From the data record we may calculate various averages that may be related to the parameters of the harmonic expansion. Thus, we find the average height  $\langle h \rangle = \frac{1}{N} \sum_{n=1}^N h_n = a_0$  because all the cosines average out to zero. Without any loss of generality we may always subtract the average water level  $a_0$  from the measured heights. Assuming from now on that  $\langle h \rangle = a_0 = 0$ , the variance of the height becomes

$$\langle h^2 \rangle = \frac{1}{N} \sum_{n=1}^N h_n^2 = \frac{1}{2} \sum_{m=1}^M a_m^2. \quad (22-80)$$

In the last step we have used that the harmonics are uncorrelated so that the average of the product of different harmonics vanishes, whereas the average of the square of any of the cosines is  $1/2$  (see problem 22.15).

For large  $N$  the frequencies constitute almost a continuum and since the energy is proportional to the square of the amplitude, the *power spectrum* of the observed waves may be defined to be

$$S(\omega_m) = \frac{N\epsilon}{4\pi} a_m^2. \quad (22-81)$$

The coefficient in front has been chosen such that for large  $N$  we may write the sum over  $m$  as an integral

$$\langle h^2 \rangle = \frac{1}{2} \sum_{m=1}^M a_m^2 \approx \int_0^{\omega_M} S(\omega) d\omega, \quad (22-82)$$

where  $d\omega = 2\pi/N\epsilon$  is the distance between neighboring frequencies.

### The “canonical” form of the spectrum

The empirical spectra have a single peak with a long tail towards higher frequencies and a sharp drop-off below. The position of the peak depends strongly on the wind velocity  $U$  whereas the high-frequency tail appears to be the same for all  $U$  (see fig. 22.8). We shall now see that it is possible to understand the general form of the spectrum using the methods of statistical mechanics.

The wind speed  $U$  sets the level of excitation of the ocean surface at large, but cannot control what happens locally so that the local wave energy  $E$  in a small neighborhood of a fixed point in principle can take any value. But because the energy has to come from the huge reservoir of wave energy in the surrounding ocean, the probability that the local energy actually gets the value  $E$  is suppressed by a canonical Boltzmann factor  $e^{-\beta E}$ , where the “inverse temperature”  $\beta$  is a measure of the level of excitation of the ocean. Multiplying with the energy per unit of frequency  $dE/d\omega$  the energy spectrum becomes

$$S \sim e^{-\beta E} \frac{dE}{d\omega}. \quad (22-83)$$

Provided the nonlinearity is not excessive, the local energy is proportional to the square of the amplitude  $E \sim a^2$ . Since the local energy cannot depend on  $U$ , the amplitude must be of magnitude  $a \sim g_0/\omega^2$ , because that is the only length scale which may be constructed from  $g_0$  and  $\omega$ . Taking  $E \sim g_0^2/\omega^4$  and normalizing the frequency in the exponent by  $g_0/U$ , we get the following model for the spectrum,

$$S(\omega) = \alpha \frac{g_0^2}{\omega^5} \exp \left[ -\beta \left( \frac{g_0}{U\omega} \right)^4 \right], \quad (22-84)$$

where  $\alpha$  and  $\beta$  are dimensionless parameters. This spectrum has indeed a sharp low-frequency cutoff, a single peak, and a high-frequency tail that is independent of  $U$  (when  $\alpha$  is independent of  $U$ ).

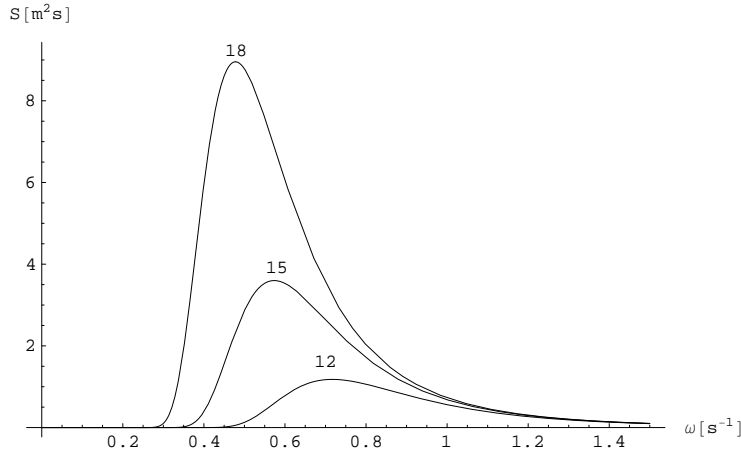


Figure 22.8: Pierson-Moskowitz wave spectrum  $S$  as a function of circular frequency  $\omega$  for three different wind speeds  $U = 10, 15, 20$  m/s. Notice that the high frequency tail is independent of  $U$ .

The root-mean-square amplitude and the peak frequency are easily evaluated,

$$\sqrt{\langle h^2 \rangle} = \sqrt{\frac{\alpha}{\beta}} \frac{U^2}{2g_0}, \quad \omega_p = \left( \frac{4\beta}{5} \right)^{1/4} \frac{g_0}{U}. \quad (22-85)$$

Notice that these quantities are scaled by the only possible combinations of  $U$  and  $g_0$  that have the right dimensions.

### The Pierson-Moskowitz empirical spectrum

Assuming that the statistical equilibrium is the same everywhere on the ocean surface, the dimensionless parameters  $\alpha$  and  $\beta$  can only depend on  $U$  and  $g_0$ , but since there is no dimensionless combination of  $U$  and  $g_0$ , both  $\alpha$  and  $\beta$  must be constants. Pierson and Moskowitz<sup>2</sup> fitted empirical spectra for a range of wind velocities and found the values

$$\alpha = 8.1 \times 10^{-3}, \quad \beta = 0.74. \quad (22-86)$$

The root-mean-square amplitude and spectrum peak position are

$$\sqrt{\langle h^2 \rangle} = 0.11 \frac{U^2}{2g_0}, \quad \omega_p = 0.88 \frac{g_0}{U}. \quad (22-87)$$

The actual spectrum is quite sensitive to the height at which the wind speed is determined because of air turbulence close to the surface. In the data used in the fit, the wind speed was measured about 20 m above the average surface level.

In fig. 22.8 the Pierson-Moskowitz spectrum is shown for three different wind speeds. One notices how the high-frequency tails coincide, and how the low-frequency cutoff becomes sharper as the wind speed increases.

<sup>2</sup>W. J. Pierson and L. Moskowitz, *J. Geophysical Research* 69, 5181 (1964); L. Moskowitz, *ibid* p. 5161; W. J. Pierson, *ibid* p. 5191.

**Example 22.7.1:** At a wind speed of  $U = 15$  m/s the period at peak is about  $\tau_p = 11$  s, corresponding to a deep-water wavelength of  $\lambda_p = 186$  m and a phase velocity of  $c_p = 17$  m/s. The average amplitude of the waves raised by this wind is  $\sqrt{\langle h^2 \rangle} = 1.2$  m. As a measure of the nonlinearity one may take  $k_p \sqrt{\langle h^2 \rangle} = 0.04$  where  $k_p = \omega_p^2/g_0 = 0.03$  m<sup>-1</sup> is the peak wave number, determined from the deep-water dispersion relation (22-24). According to this estimate, the average nonlinearity at play at this wind speed is indeed quite small.

The assumed dynamic equilibrium of the ocean surface takes a long time to develop, and more so the higher the wind speed. A wind with velocity  $U$  lasting a time  $t$  must have travelled over an upwind distance  $L = Ut$ , called the *fetch*. Even for a moderate wind at 15 m/s the sea takes about 8 hours to develop, so that the fetch is about 500 km. Since the fetch empirically grows roughly like  $U^3$ , much stronger winds in practice rarely manage to fully develop the equilibrium power spectrum of the sea because of the finite distance to the lee shore and the finite size of the weather systems generating the winds.

## Problems

**22.1** Calculate explicitly the form of a superposition of harmonic waves

$$h = \int_{-\infty}^{\infty} a(k) \cos[kx - \omega(k)t + \chi(k)] dk, \quad (22-88)$$

where

$$a(k) = \frac{1}{\Delta k \sqrt{\pi}} \exp\left(-\frac{(k - k_0)^2}{\Delta k^2}\right) \quad (22-89a)$$

$$\omega(k) = \omega_0 + c_g(k - k_0) \quad (22-89b)$$

$$\chi(k) = \chi_0 - x_0(k - k_0). \quad (22-89c)$$

Describe its form and determine what  $x_0$  represents. Hint: write the wave as the real part of a complex wave and use the known Gaussian integrals.

**22.2** Check whether the shallow-wave solution (22-35) actually satisfies the field equations (22-15). Discuss what is wrong, if they do not.

**22.3** Show that the fluid particles move in ellipses in a flat-bottom gravity wave, and that the ellipses become flat close to the bottom. What happens in the deep-water limit?

**22.4** Show that the depth at which non-linear effects become important in waves rolling up on a gently sloping beach is of order of magnitude,

$$d \approx a_0^{4/5} d_0^{1/5} \quad (22-90)$$

where  $a_0$  and  $d_0$  is the amplitude and depth at the beginning of the beach.

**22.5** Define the depth-averaged velocity for a small-amplitude gravity wave,

$$\bar{v}_x = \frac{1}{d+h} \int_{-d}^h v_x dz \quad (22-91)$$

Show that in the leading approximation its time average is

$$\langle \bar{v}_x \rangle = \frac{g_0 a^2}{2cd} \left(1 - \frac{c^2}{g_0 d}\right) \quad (22-92)$$

What happens in the flat-water limit?

**22.6** Calculate the ratio between the amount of water transported during a period and the total amount of water in a shallow-water wave. Estimate its typical value.

\* **22.7** There is a small subtlety in the derivation of the average mass transport in a wave (22-40), because the leading (sloshing term) could have corrections of order  $h$ . Show that for any kind of potential flow  $\mathbf{v} = \nabla \Psi$  with periodic velocity potential  $\Psi = \Psi(kx - \omega t, z)$ , the average transport rate will always be

$$\langle Q \rangle = -\rho_0 L \langle h v_x \rangle_{z=h} \quad (22-93)$$

in the small amplitude limit. Hint: Use that the average over a period is equivalent to an average over a wavelength.

- \* **22.8** In the derivation of (22-50) there is a subtlety in the use of momentum transport instead of the proper pressure force acting on a vertical cut through the wave

$$\mathcal{F}_x = - \int_{-d}^h p L dz \quad (22-94)$$

Show that in potential flow, its average equals the average rate of momentum transport,

$$\langle \mathcal{F}_x \rangle = \left\langle \int_{-d}^h \rho_0 v_x^2 L dz \right\rangle \quad (22-95)$$

Hint: Include the quadratic terms.

- 22.9** Consider a small-amplitude gravity line wave and

(a) Show that

$$v_x^2 + v_z^2 = \nabla_x(\Psi v_x) + \nabla_z(\Psi v_z) \quad (22-96)$$

(b) Show that the time average satisfies

$$\langle v_x^2 + v_z^2 \rangle = \nabla_z \langle \Psi v_z \rangle \quad (22-97)$$

(c) Use this to calculate the kinetic energy (22-45).

- 22.10** Prove the virial theorem

$$\langle T \rangle = \frac{n}{2} \langle \mathcal{V} \rangle \quad (22-98)$$

for a single particle in periodic motion in a power potential  $\mathcal{V} = kr^n$ .

- 22.11** Justify qualitatively the common observation that waves rolling towards a beach tend to straighten out so that the wave crests become parallel to the beach.

- 22.12** For what size raindrop will the pressure due to surface tension equal atmospheric pressure?

- 22.13** a) Determine where the phase and group velocities (22-25) for deep-water waves cross (use  $\alpha = 0.073$  N/m) and the common value at the crossing. b) Determine the minimal value of the phase velocity and the corresponding wavelength .

- 22.14** A square jar is half filled with water of density  $1 \text{ g/cm}^3$  lying below oil of density  $0.8 \text{ g/cm}^3$ . The interface has surface tension  $0.3 \text{ N/m}$ . Determine the largest horizontal size of the jar which permits the oil to be stably above the water.

**22.15 Discrete Fourier transformation.**

Assume that a set of  $N$  generally complex numbers  $h_n$  numbered  $n = 0, 1, 2, \dots, N-1$ .  
 1. Define the Fourier coefficients

$$\hat{h}_m = \frac{1}{\sqrt{N}} \sum_{n=0}^{N-1} h_n \exp \left[ 2\pi i \frac{nm}{N} \right] \quad (22-99)$$

(a) Show that

$$\sum_{m=0}^{N-1} \exp \left[ 2\pi i \frac{nm}{N} \right] = \begin{cases} N & \text{for } n = 0 \\ 0 & \text{for } 1 < n < N \end{cases} \quad (22-100)$$

(b) Show the reciprocity theorem

$$h_n = \frac{1}{\sqrt{N}} \sum_{m=0}^{N-1} \hat{h}_m \exp \left[ -2\pi i \frac{nm}{N} \right] \quad (22-101)$$

(c) Show Parseval's theorem

$$\sum_{n=0}^{N-1} |h_n|^2 = \sum_{m=0}^{N-1} |\hat{h}_m|^2 \quad (22-102)$$

(d) Assume from now on that that  $h_n$  is real. Show that

$$\hat{h}_m^\times = \hat{h}_{-m} \quad (22-103)$$

where  $\hat{h}_{-m}$  means  $\hat{h}_{N-1-m}$ .

(e) Put

$$\hat{h}_0 = \sqrt{N} a_0 \quad \hat{h}_m = \frac{1}{2} \sqrt{N} a_m e^{i\chi_m} \quad (22-104)$$

where  $a_n$  and  $\chi_n$  are real. Show that  $a_{-n} = a_n$  and  $\chi_{-n} = -\chi_n$ . Show that for odd  $N = 2M + 1$

$$h_n = a_0 + \sum_{m=1}^M a_m \cos(\omega_m t_n - \chi_m) \quad (22-105)$$

where  $t_n = n\epsilon$ , and  $\omega_m = 2\pi m/N\epsilon$ .

(f) Show that

$$\frac{1}{N} \sum_{n=0}^{N-1} (h_n - a_0)^2 = \frac{1}{2} \sum_{m=1}^M a_m^2 \quad (22-106)$$

